Journal of Neurotrauma

DOI: 10.1089/neu.2017.5203

Traumatic brain injury in hTau model mice: Enhanced acute macrophage response and altered long-term recovery

Authors:

Olga N. Kokiko-Cochran[1*], Maha Saber[2], Shweta Puntambekar[3], Shane Bemiller[3], Atsuko Katsumoto[3], Yu-Shang Lee[4], Kiran Bhaskar[5], Richard M. Ransohoff[6], Bruce T. Lamb[3]

Affiliations:

[1]Dept. of Neuroscience, The Ohio State University, College of Medicine, Columbus, OH, USA.

[2]The University of Arizona, College of Medicine, Phoenix, AZ, USA.

[3]Medical and Molecular Genetics, Stark Neuroscience Research Institute, Indiana University, Indianapolis, IN, USA.

[4]Dept. of Neuroscience, Lerner Research Institute, Cleveland Clinic, Cleveland, OH, USA

[5]Dept. of Molecular Genetics Microbiology and Neurology, University of New Mexico, Albuquerque NM, USA.

This is the author's manuscript of the article published in final edited form as:

Kokiko-Cochran, O. N., Saber, M., Puntambekar, S., Bemiller, S. M., Katsumoto, A., Lee, Y.-S., … Lamb, B. T. (2017). Traumatic brain injury in hTau model mice: Enhanced acute macrophage response and altered long-term recovery. Journal of Neurotrauma. https://doi.org/10.1089/neu.2017.5203

[6]Neuroimmunology, Acute Neurology and Pain Research and Early Discovery Unit, Biogen, 02142, Cambridge, MA, USA.

*Corresponding author

Running Title: Human tau alters recovery from TBI

Table of Contents Title: Wild-type human tau alters recovery from TBI in mice

Key Words: Traumatic brain injury, microtubule associated protein tau (MAPT), neuroinflammation, spatial memory

Author Contact Information:

Olga N. Kokiko-Cochran, Ph.D.

Department of Neuroscience

The Ohio State University

257 Institute for Behavioral Medicine Research Bld.

460 Medical Center Dr.

Columbus, OH 43210

Phone: 614-366-3642

Email: olga.kokiko-cochran@osumc.edu

Maha Saber, Ph.D.

The University of Arizona

College of Medicine

550 East Van Buren St.

Phoenix, AZ 85004

Phone: 602-827-2348

Email: saberm@Arizona.email.edu

Shweta Puntambekar, Ph.D.

Medical and Molecular Genetics

Stark Neuroscience Research Institute

Indiana University

320 West 15th Street

Indianapolis, IN 46202

Phone: 317-278-5811

Email: sspuntam@iu.edu

Shane Bemiller, Ph.D.

Medical and Molecular Genetics

Stark Neuroscience Research Institute

Indiana University

Journal of Neurotrauma
Traumatic brain injury in hTau model mice: Enhanced acute macrophage response and altered long-term recovery
 (DOI: 10.1089/neu.2017.5203)
This paper has been peer-reviewed and accepted for publication, but has yet to undergo copyediting and proof correction. The final published version may differ from this proof.

320 West 15th Street

Indianapolis, IN 46202

Phone: 317-278-5811

Email: sbmille@iu.edu

Atsuko Katsumoto, M.D., Ph.D.

Medical and Molecular Genetics

Stark Neuroscience Research Institute

Indiana University

320 West 15th Street

Indianapolis, IN 46202

Phone: 317-278-5811

Email: akatsumo@iu.edu

Yu-Shang Lee, Ph.D.

Department of Neuroscience

Lerner Research Institute

Cleveland Clinic

9500 Euclid Avenue

Cleveland, OH 44195

Phone: 216-445-5040

Email: leey2@ccf.org

Kiran Bhaskar, Ph.D.

Molecular Genetics and Microbiology

MSC08 4660

1 University of New Mexico

Albuquerque, NM 87131-0001

Phone: (505) 272-1230

Email: kbhaskar@salud.unm.edu

Richard M. Ransohoff, M.D.

Biogen

225 Binney St.

Cambridge, MA 02142

Phone: 617-914-4662

Email: richard.ransohoff@biogenidec.com

Bruce T. Lamb, Ph.D.

Medical and Molecular Genetics

Stark Neuroscience Research Institute

Indiana University

320 West 15th Street

Indianapolis, IN 46202

Phone: 317-278-5811

Email: btlamb@iu.edu

Journal of Neurotrauma
Traumatic brain injury in hTau model mice: Enhanced acute macrophage response and altered long-term recovery
 (DOI: 10.1089/neu.2017.5203)
This paper has been peer-reviewed and accepted for publication, but has yet to undergo copyediting and proof correction. The final published version may differ from this proof.

Journal of Neurotrauma
Traumatic brain injury in hTau model mice: Enhanced acute macrophage response and altered long-term recovery
 (DOI: 10.1089/neu.2017.5203)
This paper has been peer-reviewed and accepted for publication, but has yet to undergo copyediting and proof correction. The final published version may differ from this proof.

Abstract

TBI induces widespread neuroinflammation and accumulation of microtubule associated protein tau (MAPT) - two key pathological features of tauopathies. This study sought to characterize the microglial/macrophage response to TBI in genomic-based *MAPT* transgenic mice in a *Mapt* knockout background (called hTau). Two-month-old hTau and age-matched control male and female mice received a single lateral fluid percussion TBI or sham injury. Separate groups of mice were aged to an acute (3 days post-injury [DPI]) or chronic (135 DPI) post-injury time point. As judged by tissue immunostaining for macrophage markers, microglial/macrophage response to TBI was enhanced at 3 DPI in hTau mice compared to control TBI and sham mice. However, MAPT phosphorylation increased in hTau mice regardless of injury group. Flow cytometric analysis revealed distinct populations of microglia and macrophages within all groups at 135 DPI. Unexpectedly, microglial reactivity was significantly reduced in hTau TBI mice compared to all other groups. Instead, hTau TBI mice showed a persistent macrophage response. In addition, TBI enhanced MAPT pathology in the temporal cortex and hippocampus of hTau TBI mice compared to controls 135 DPI. A battery of behavioral test revealed that TBI in hTau mice resulted in compromised use of spatial search strategies to complete a water maze task despite lack of motor or visual deficits. Collectively, these data indicate that the presence of wild-type human tau alters the microglial/macrophage response to a single TBI, induces delayed, region-specific MAPT pathology, and alters cognitive recovery; however, the causal relationship between these events remains unclear. These results highlight the potential significance of communication between MAPT and microglia/macrophages following TBI and emphasize the role of neuroinflammation in post-injury recovery.

Introduction

Traumatic brain injury (TBI) has been implicated as one of the most significant environmental risk factors for Alzheimer's disease (AD), Parkinson's disease (PD) and frontotemporal dementia (FTD). The cumulative effect of multiple brain injuries is also highlighted by the prevalence of chronic traumatic encephalopathy (CTE) in professional athletes.[1–4] Key pathological features of neurodegenerative tauopathies include neuroinflammation, hyperphosphorylation and aggregation of microtubule associated protein tau (MAPT), and formation of neurofibrillary tangles (NFTs).[5] Given that a primary TBI is irreversible, increased attention has been directed toward identifying secondary injury mechanisms facilitating neurodegeneration. Axonal injury following the initial insult is proposed to be the first perturbation of MAPT as it promotes microtubule dissociation and subsequent phosphorylation and aggregation.[3,6,7] A robust and persistent post-injury neuroinflammatory response may then be sufficient to exacerbate tau pathology and promote neurodegeneration.

Post-injury neuroinflammation is characterized by activation of brain-resident microglia, infiltration of peripheral myeloid cells (PMCs) due to disruption of the blood-brain-barrier (BBB), astrogliosis and increased synthesis and release of pro- and anti-inflammatory molecules.[8,9] Several observations suggest that TBI-induced neuroinflammation regulates MAPT pathologies, including hyperphosphorylation and aggregation. First, a recent set of experiments demonstrated that MAPT pathology temporally co-exists with gliosis following repetitive mTBI in the hTau mouse model of MAPT pathology.[10] Similar findings have been reported in wild-type mice after blast-induced TBI and in a triple transgenic mouse model of AD following a single moderate TBI.[2,11] Second, numerous reports have demonstrated activated microglia near the injury release several pro-inflammatory cytokines and chemokines and that these inflammatory molecules in turn can exacerbate MAPT pathologies.[10,12,13] Finally, previous work from our group revealed that targeted modulation of key chemokines involved in the post-inflammatory response significantly influences AD-like neuropathology following mild TBI. Specifically, interruption of CCR2 signaling through the use of *Ccr2$^{RFP/RFP}$ deficient mice reduced post-injury monocytic infiltration and axonal pathology but enhanced cortical and hippocampal MAPT mislocalization and hyperphosphorylation.*[14]

Journal of Neurotrauma
Traumatic brain injury in hTau model mice: Enhanced acute macrophage response and altered long-term recovery
 (DOI: 10.1089/neu.2017.5203)
This paper has been peer-reviewed and accepted for publication, but has yet to undergo copyediting and proof correction. The final published version may differ from this proof.

We sought to extend these findings by examining the effects of a single TBI in a disease-relevant mouse model of tauopathy. We utilized genomic-based *MAPT* transgenic mice (line 8c) in a *Mapt* knockout background (called "hTau") that express all six isoforms of non-mutant human MAPT. Notably, the mouse brain contains only 4 repeat (4R) MAPT isoforms, but the human brain contains an equal distribution of both 3 repeat (3R) and 4R MAPT isoforms. Naïve hTau mice display somato-dendritic MAPT redistribution at 3 months of age, MAPT hyperphosphorylation at 6 months of age, MAPT aggregation at nine-months of age, and neuronal loss by 15 months of age. Thus, the pathology in hTau mice is not completely related to an overexpression of human MAPT, but instead is a result of an altered ratio of 3R isoforms over 4R isoforms that is not present in line 8c alone.[15–18]

At two-months of age, hTau and C57BL/6J (B6) mice were exposed to lateral fluid percussion TBI or sham injury and examined at both acute and chronic time points. Since TBI induces microglial reactivity as well as peripheral macrophage recruitment that correlate with MAPT pathology,[2,11–13,19,20] we focused our efforts on quantifying the microglial and macrophage response to TBI. We also evaluated the spatial and temporal distribution of MAPT pathology and documented behavioral changes as subjects aged. Our group has utilized these hTau mice in various recent studies and clearly demonstrated that reactive microglia are critical mediators of MAPT pathology.[21–24] Notably, the microglial/macrophage response to TBI was enhanced in hTau mice compared to all other groups at 3 days post-injury (DPI) and hTau mice showed increased MAPT phosphorylation in the ipsilateral temporal cortex. Through flow cytometric analysis we identified four, unique myeloid populations that persist in the brain at 135 DPI. Based on CD45 expression we conclude that there is an overall reduction in microglial reactivity with a persistent macrophage presence in hTau TBI mice compared to other control groups, which corresponded with an increase in region-specific MAPT pathology and cognitive dysfunction. Collectively, these data show that a single TBI alters the neuroinflammatory environment, advances the appearance of age-related MAPT pathology and induces behavioral impairment in a humanized mouse-model of tauopathy; however, the mediating mechanisms in this relationship require further investigation.

Materials and Methods

Study Design

The primary objective of this study was to characterize the post-injury microglial/macrophage response to TBI at both acute and chronic time points in the presence or absence of wild-type human tau. Separate groups of hTau and B6 mice were used for acute and chronic studies. Each subject was randomized to the TBI or sham group following surgical preparation. A separate investigator blinded to experimental group performed subsequent data analysis. All subjects surviving to 3 or 135 DPI were included in data analysis and no outliers were excluded.

Mice

The hTau mouse model of tauopathy was utilized to characterize recovery following TBI.[15] Two-month old hTau mice (mixed sex; n = 10-12 mice per group) maintained on the C67BL/6J genetic background were used for all studies. Age- and sex-matched B6 animals served as controls for all studies. Animals were housed at the Cleveland Clinic Biological Resources Unit. The Institutional Animal Care and Use Committee (IACUC) of the Cleveland Clinic approved all animal procedures.

Surgical preparation and injury.

All surgical procedures were completed as previously described.[25] Briefly, two-month-old hTau and B6 mice were anesthetized with a combination of ketamine (100 mg/kg) and xylazine (10 mg/kg) before being placed in a stereotaxic frame. Bupivicaine (0.25%, 50 μl) was delivered subcutaneously before midline incision. A 3.0 mm craniotomy was trephined over the right parietal cortex midway between bregma and lambda leaving the dura intact. A modified Leur-Loc syringe (3.0 mm inside diameter) was placed over the exposed dura and held in place by cyanoacrylate adhesive. Mice were placed on a heating pad to recover following surgical preparation. Once animals regained normal ambulatory behavior, they were placed in their home cage overnight. Twenty-four hours after surgical preparation, all mice were anesthetized with the same combination of ketamine and xylazine and connected to the FPI device (Amscien Instruments, Richmond, VA). A moderate level FPI (*M* = 1.0 atmospheres of extracranial pressure) was delivered to animals in the TBI group. Animals in the sham group were connected to the injury device; however, no fluid pulse was delivered. The syringe and adhesive were removed from the skull following FPI or

Journal of Neurotrauma
Traumatic brain injury in hTau model mice: Enhanced acute macrophage response and altered long-term recovery
 (DOI: 10.1089/neu.2017.5203)
This paper has been peer-reviewed and accepted for publication, but has yet to undergo copyediting and proof correction. The final published version may differ from this proof.

sham injury and the incision was sutured closed. All animals recovered on a heating pad before being placed in their home cage. Mice were sacrificed at either 3 DPI or 135 DPI (one week after completion of spatial memory testing in the water maze).

Immunohistochemistry.

Half of the mice in each group (*n* = 5-6 per group) were deeply anesthetized with ketamine (100 mg/kg) and xylazine (10 mg/kg) and transcardially perfused with ice-cold 0.1 mol/L sodium phosphate buffer at 3 DPI and 135 DPI. Whole brain samples were removed from the cranium and drop-fixed in 4% paraformaldehyde in PBS and stored at 4°C. Following cryoprotection in 30% sucrose/PBS, brains were embedded in optimal cutting temperature (OCT) compound and subsequently cut into free floating 30 µm coronal sections for neuropathological analysis. The following dilutions were used for primary antibodies: CD45 (Serotec) 1:500; F4/80 (Serotec) 1:500; CD68 (Abcam); AT180 (pThr231, Pierce); all incubated at 4°C overnight followed by secondary antibodies conjugated to biotin (Vector Laboratories; 1:200). Sections incubated with Avidin/Biotinylated enzyme complex (ABC reagent, Vector Laboratories; for immunohistochemistry) reagent for 1 hour at room temperature following by 3-3'-diaminobenzidine (DAB; Vector Laboratories) until a brown reaction was observed. Silver staining was performed on 30µm coronal brain sections using a commercially available FD NeuroSilver II kit according to manufacturer's instructions.

Isolation of microglia and monocytes and flow cytometry.

At 135 DPI mice from each experimental group were deeply anesthetized with ketamine (100 mg/kg) and xylazine (10 mg/kg) and transcaridally perfused with 1x Hank's balanced salt solution (HBSS). Brains were removed, chopped, and digested using the Macs Neural tissue dissociation kit (Miltenyl Biotec). Following a wash, digested tissue was resuspended in 30% Percoll and overlayed with 1mL of 10% fetal bovine serum in Roswell Park Memorial Institute (RPMI)-media. Samples were placed in a centrifuge for 15 minutes at 800g with no brake. Myelin and buffer were aspirated off the cells of interest, which settled at the bottom of the tube during centrifugation. Finally, the cells were resuspended in FACS buffer (PBS containing BSA and sodium azide)/FC block for 5 minutes at room temperature. The following antibodies were used for cell surface staining of isolated microglia and monocytes: anti-mouse CD45-APC (BioLegend, 1:500), anti-mouse CD11b-

BV605 (BioLegend, 1:100), anti-mouse Ly6C-FITC, 1:100). Flow cytometry was performed with a BD LSR Fortessa (BD Bioscience) and analyzed using FlowJo software (version 9.3.1, TreeStar, Inc. Ashland, OR).

Behavioral Assessment. All behavioral tests were completed as previously described.[26]

Rotarod. Balance and coordination was assessed with a standard rotarod test (Rotamex, Columbus Instruments). All mice received baseline training before surgical preparation, and post-injury testing was completed at 1, 3, 6, 30, 60, and 90 DPI. Each testing day included three five-minute trails in which rod rotation increased from 4 rotations per minutes (RPM) to 30 RMP. Average latency to fall was calculated for each testing day and compared between groups.

Y maze. Time dependent changes in spatial working memory were evaluated in the y maze. Briefly, each mouse completed one five-minute trial at 7, 30, 60, and 90 DPI. Following placement in the center of the maze, a mouse had free access to all three arms. Total arm entries and spontaneous alternation between arms was recorded for each testing day and compared between groups.

Water maze. A standard version of the water maze was used to assess spatial learning and reference memory beginning 120 DPI. During visible platform training, animals were placed in the pool at one of four start locations and given 60 seconds to locate a visible goal platform that was placed in a new location for each trial. After three days of training, the water level was increased two centimeters to “hide” the goal platform, which then remained in the same location for five days of memory testing. Constant spatial cues around the pool served as guides for the animals to locate the submerged goal platform. Animals remained on the platform for 15 seconds after 60 seconds elapsed or after they located the platform on their own. A single probe trial, in which the goal platform was removed, was completed at 129 DPI approximately 24 hours after the last memory trial. Mice were sacrificed the following week at 135 DPI. All trials were analyzed with EthoVision XT (Noldus) video tracking software. Primary dependent variables of interest were latency to reach the goal platform, time spent in each quadrant, and swim speed. Swim pattern was subsequently analyzed by an experimenter blinded to experimental groups and based on previously reported strategies which included identification of spatial, non-spatial, and circling search strategies.[27]

Journal of Neurotrauma
Traumatic brain injury in hTau model mice: Enhanced acute macrophage response and altered long-term recovery
 (DOI: 10.1089/neu.2017.5203)
This paper has been peer-reviewed and accepted for publication, but has yet to undergo copyediting and proof correction. The final published version may differ from this proof.

Statistical analysis.

All statistical analysis was completed with GraphPad Prism 6.07 or IBS SPSS Statistics 24. A mixed model factorial analysis of variance (ANOVA) was used to evaluate group differences. ANOVA with repeated measures was used to classify group differences in behavioral tests. The between factors were genotype and injury and the within-group factor was day of testing. Main effects and interaction effects were considered. Two-tailed Students *t* test was utilized for post-hoc comparison of the main effect(s) between B6 and hTau mice. *t* test with Welch's correction was incorporated to address comparisons in which the two samples had unequal variances or an unequal number of samples. Statistical significance was determined at $p < 0.05$. All data are presented as mean ± standard error of the mean (SEM).

Results

Microglial/Macrophage Response to TBI is Enhanced in hTau Mice at 3 DPI.

TBI induces a widespread neuroinflammatory response characterized by microglial reactivity, monocyte infiltration and increased production and release of inflammatory mediators.[19] CD45 is a type 1 transmembrane protein present on all hematopoietic cells that is upregulated in activated macrophages and expressed at lower levels in brain resident microglia.[28] Consistent with our previous findings,[25,26] brain injury resulted in increased CD45 immunoreactivity near the injury site in B6 and hTau mice at 3 DPI (Fig. 1A). Two-way ANOVA revealed a significant genotype effect and injury effect in the cortex lateral to the injury site. T test (with Welch's correction) confirmed that CD45 immunoreactivity was increased in hTau TBI mice compared to B6 TBI mice in the lateral cortex (Fig. 1F). A similar effect was detected in the ipsilateral hippocampus (Fig. 1D) with CD45 immunoreactivity significantly increased in hTau TBI mice compared to B6 TBI mice in the ipsilateral hippocampus (Fig. 1G). These findings indicate that the presence of wild-type human tau significantly increases the acute microglial and macrophage response to TBI; however, the cell specific contribution to CD45 immunoreactivity could not be distinguished through immunohistochemistry.

Quantification of percent area covered by F4/80 immunohistochemistry supported the altered microglial/macrophage response in hTau TBI mice. F4/80 is a cell surface glycoprotein highly expressed on mouse macrophages.[29] Two-way ANOVA revealed a significant injury effect and interaction effect in the cortex lateral to the injury site (Fig. 1B). hTau TBI mice displayed enhanced F4/80 immunoreactivity compared to B6 TBI mice; however, a statistically significant genotype effect was not observed (Fig. 1F). Similarly, two-way ANOVA revealed an injury effect in F4/80 immunoreactivity in the ipsilateral hippocampus (Fig. 1E, 1G).

Finally, CD68 immunoreactivity was used to identify macrophages, including microglia-derived macrophages responding to TBI or sham injury at 3 DPI. CD68 is a highly glycosylated transmembrane protein regarded as a potential marker for phagocytic activity in tissue macrophages.[30] Consistent with our previous results,[25] CD68 immunoreactivity was localized to the cortex at 3 DPI and not apparent in subcortical structures such as the hippocampus (Fig. 1C). A significant effect of injury was detected with two-way ANOVA. Consistent with CD45 and F4/80, hTau TBI mice displayed increased CD68 expression compared to B6 TBI mice (Fig. 1F). Collectively, these data confirm that the microglial and/or macrophage response to brain injury is enhanced in hTau mice compared to B6 control mice.

TBI Induces Region Specific MAPT Phosphorylation in hTau Mice Compared to B6 Mice at 3 DPI.

To test whether enhancing microglial/macrophage reactivity in hTau mice promotes MAPT hyperphosphorylation, injured and sham brain tissue from B6 and hTau mice was immunostained with AT180 antibody. TBI and sham injury increased hyperphosphorylation at the phosphor-thr231 (AT180) epitope in the ipsilateral temporal cortex in hTau mice compared to B6 mice (Fig. I-J). No significant differences were observed in AT180 immunoreactivity in the lateral cortex near the site of injury (Fig. 1H), although a trend toward an interaction effect was detected (p = 0.09, Fig. 1J). These results suggest that MAPT phosphorylation is not restricted to the site of TBI or sham injury, and even distal brain regions are vulnerable to damage.

TBI Promotes a Distinct Microglial/Macrophage Phenotype in hTau TBI Mice at 135 DPI.

To document the long-term consequences of TBI in hTau mice, separate groups of hTau and B6 mice received TBI or sham injury at two-months old and aged 135 DPI. CD45 immunoreactivity was variable within groups by 135 DPI and the rod-shaped morphology of CD45+ cells in TBI mice was less apparent compared to 3 DPI (Fig. 2A). Quantification of percent area covered by CD45 immunoreactivity in the cortex lateral to the site of injury verified no significant differences between groups (Fig. 2C). CD45 immunoreactivity was not quantified in the ipsilateral hippocampus at 135 DPI due to low levels of detection; however, several CD45+ cells were identified in the optic tract of brain injured mice. Subsequent quantification of percent area covered by CD45 immunoreactivity in the optic tract revealed no significant differences between groups (Fig. 2B-C).

Mononuclear cells isolated from whole brains of TBI and sham injured B6 and hTau mice at 135 DPI were analyzed using flow-cytometry to distinguish populations of $CD45^{low/+}$ microglia and $CD45^{high}$ peripheral lymphocytes and myeloid cells (Fig 3A). While the peripheral macrophages were a single population of $Ly6C^{+}CD11b^{+}CD45^{high}$ cells (Fig 3B), brain resident microglia could be subdivided into several populations. At 135 DPI, $CD45^{low/+}$ microglia displayed distinct sup-populations of $CD11b^{low}$ and $CD11b^{high}$ cells (Fig 3B). A third population of $CD45^{int}$ microglia was identified, which expressed CD45 at levels that were higher than the $CD11b^{low}$ and $CD11b^{high}$ microglia (Fig 3B-C). Thus, based on CD45 expression, we identified four, unique myeloid populations that persist under chronic injury conditions. The $CD11b^{low}$ microglia expressed the lowest levels of CD45, followed by the $CD11b^{high}$ and the $CD45^{int}$ group characteristic of reactive microglia, while the peripheral macrophages were the highest expressers of CD45 (Fig 3C).

Quantitation of microglial response revealed a significant reduction in the proportion of all three subpopulations in the hTau TBI group as compared to the B6 TBI cohort (Fig 3D). No significant differences were seen in the proportions of $CD11b{+}CD45^{high}$ cells (Fig 3F). Analysis of inflammatory activation showed the presence of $Ly6c^{low}$ and $Ly6c^{high}$ cells in the $CD11b{+}CD45^{int}$ microglia and the $CD11b{+}CD45^{high}$ macrophages. Interestingly, while $Ly6c^{low}$ and $Ly6c^{high}$ microglia are significantly reduced in the hTau TBI mice (Fig 3E), $Ly6c^{low}$ macrophages persist at significantly higher numbers as compared to the hTau sham injured group (Fig 3G). These results suggest that a single TBI significantly

changes the proportion of reactive microglia and macrophages within the brains of hTau mice compared to B6 mice.

Region Specific MAPT Pathology Persists in hTau TBI Mice at 135 DPI

Given the unique pattern of microglial and macrophage reactivity following TBI, we next examined the spatial distribution of MAPT pathology at 135 DPI in B6 and hTau mice. Naïve hTau mice display age-associated MAPT pathology, beginning with somato-dendritic MAPT accumulation and hyperphosphorylation around 3-4 months of age and subsequent MAPT aggregation around 10 months of age.[15] Thus, we expected hTau sham and TBI mice to have some age-related MAPT pathology but predicted that it would be enhanced after brain injury. AT180 immunoreactivity was detected in all groups at 135 DPI and increased expression was notable in the cortex lateral to the site of injury as well as in the ipsilateral temporal cortex in hTau TBI mice (Fig. 2D-E). Two-way ANOVA of percent area covered by AT180 immunoreactivity revealed a significant genotype effect in the cortex lateral to the site of injury and in the ipsilateral temporal cortex (Fig. 2F). AT180 immunoreactivity was highest in cortex lateral to the site of injury and in the ipsilateral temporal cortex in hTau TBI mice compared to all other groups. A significant difference in AT180 immunoreactivity was detected between B6 and hTau TBI mice in the ipsilateral temporal cortex, but no difference was detected between hTau TBI and hTau sham mice (Fig. 2F). Together, these data indicate that MAPT phosphorylation occurs in a region dependent manner at a chronic post-injury time point following TBI in hTau mice.

To confirm and extend these results to determine if the hyperphosphorylated MAPT has acquired pre-tangle/NFT conformation, Gallyas silver staining was performed. Gallyas silver staining is a standard detection method of MAPT pathology[31] and has been utilized by our group previously in hTau mice.[21] Strikingly, numerous Gallyas-positive neurons were identified in the CA1 region of the ipsilateral hippocampus in hTau TBI mice but not in age-matched B6 or hTau control mice (Fig. 2G). Two-way ANOVA of relative number of Gallyas silver+ cells revealed a significant genotype, hemisphere and interaction effect in the hippocampus of TBI mice (Fig. 2G). Sham mice were not included in the analysis due to very few numbers of Gallyas silver+ cells. Together, these data indicate that a single TBI induces accumulation of significantly more Gallyas silver+ cells in the ipsilateral

Journal of Neurotrauma
Traumatic brain injury in hTau model mice: Enhanced acute macrophage response and altered long-term recovery
 (DOI: 10.1089/neu.2017.5203)
This paper has been peer-reviewed and accepted for publication, but has yet to undergo copyediting and proof correction. The final published version may differ from this proof.

hippocampus of hTau TBI mice than B6 TBI mice. MAPT aggregates do not typically appear in hTau mice until around 9 months of age, thus these data suggest that a single TBI accelerates MAPT aggregation in hTau mice in a region dependent manner.

TBI Induces Spatial Memory Alterations in the Absence of Motor Dysfunction in hTau TBI Mice.

Behavioral impairment has been reported at 12 months of age in naïve hTau mice, which is approximately 3 months after the first MAPT aggregates appear.[16] B6 and hTau mice completed motor and cognitive testing following TBI or sham injury as they aged to 135 DPI. Given the altered microglial/macrophage response and region specific tau pathology in hTau TBI mice, we predicted that cognitive impairment would also be advanced by 135 DPI. The rotarod test was used to examine motor function, including balance and coordination. In agreement with our previous findings,[25,26] all mice performed similarly during baseline training and at all post-injury time points. Although hTau sham mice spent less time on the rotating rod during the acute phase of testing, no significant difference were detected with repeated measures ANOVA (Fig. 4A). Spatial working memory was evaluated in the Y maze. Consistent with our previous work,[25] a significant decrease in arm entries was detected across time, $p < 0.001$(Fig. 4B). Repeated exposure to the Y maze results in decreased exploratory interest and consequently fewer arm entries. Percent spontaneous alternation was calculated by taking an average of the total number of alternations over the maximum number of alternations (total arm entries – 2). No significant differences in spontaneous alternation between arms were detected between groups at any post-injury time (Fig. 4C). Taken together, these data demonstrate that this severity of TBI does not induce global motor or cognitive deficits over time.

Water maze testing began 120 DPI. No significant differences in visible platform training were detected between groups. This finding indicated that visual deficiencies did not interfere with any subject's ability to learn the procedures of the task (i.e., swim to the platform and stay there for 15 seconds). Repeated measures ANOVA revealed a significant effect of testing day and injury group, $p < 0.01$. Neuman-Keuls multiple comparisons test indicated that latency to reach the submerged goal platform was significantly different between groups on memory testing day 1. hTau TBI mice took significantly longer to reach

the goal platform than B6 TBI and B6 sham mice, $p < 0.05$ (Fig. 4D). The statistically significant difference between groups did not persist over time as all groups displayed decreased latency to reach the goal platform across testing days. No significant differences between groups were detected in average swim speed (Fig. 4E) or average time spent in the goal quadrant during probe testing (Fig. 4F). Together, these data suggest that hTau TBI mice are deficient in acquiring the memory portion of this cognitive assessment. Although statistically significant group differences did not persist across testing days, latency to reach the goal platform remained elevated in hTau TBI mice compared to other groups. This was not related to visual or motor deficits and did not prevent hTau TBI mice from completing the task.

In an effort to better characterize group differences that contributed to an acquisition deficit in memory testing, we evaluated search strategy to find the submerged goal platform as previously described.[27] Manual categorization of search strategy in each memory testing trial was completed by a single investigator blinded to injury group. Videos of each trial were replayed in Ethovision at 2x the speed, which resulted in a timely reanalysis of swim path. A single search strategy that best described the majority of swim path was noted for each trial. Three categories of swim path were considered, including spatial, non-spatial, and looping as previously defined (Fig. 5A).[27] Briefly, spatial strategies included swimming directly to the platform (spatial direct), swimming toward the platform with only one loop (spatial indirect), and intentional searching within the goal quadrant (focal correct). Non-spatial strategies included searching the tank interior without spatial bias (scanning), searching the entire tank without spatial bias (random) and intentional searching of a portion of the tank that did not include the goal quadrant (focal incorrect). Finally, looping strategies included circular swimming at a fixed distance from the wall (chaining), circling around the outer 15 cm of the pool including thigmotaxis (peripheral looping) and swimming in tight circles with directional movement (circling).

Percentage of trials using each search strategy as a function of injury group and day of hidden platform testing is displayed in Fig. 5B-E. Several notable differences between injury groups emerged. For example spatial search strategies were utilized by hTau TBI mice far less than any other group. Compared to B6 TBI mice, hTau TBI mice displayed a preferential use of non-spatial search strategies. In addition, looping strategies made up a

Journal of Neurotrauma
Traumatic brain injury in hTau model mice: Enhanced acute macrophage response and altered long-term recovery
 (DOI: 10.1089/neu.2017.5203)
This paper has been peer-reviewed and accepted for publication, but has yet to undergo copyediting and proof correction. The final published version may differ from this proof.

larger percentage of trials in hTau mice compared to B6 mice, and use of looping strategies increased in hTau mice across testing days compared to B6 mice. This was most apparent on the last day of memory testing (day 5) when latency to reach the goal platform was similar between groups. For subsequent statistical analysis, average percentage of trials using each search strategy was calculated and compared between groups. Two-way ANOVA revealed a significant genotype effect for use of the spatial indirect search strategy, $p < 0.05$ (Fig. 5F), scanning strategy, $p = 0.05$ (Fig. 5G), and circling strategy, $p < 0.05$ (Fig. 5H). Subsequent *t* tests revealed statistically significant differences between B6 and hTau TBI mice in scanning and circling strategies; however, significant differences were also detected between B6 TBI and hTau sham mice ($p < 0.05$) confirming a primary effect of genotype. A statistically significant difference is use of spatial indirect strategy was detected between B6 and hTau TBI mice, $p < 0.01$; however, no significant difference was observed between any other groups. Collectively, these data suggest that TBI in hTau mice compromises the use of spatial search strategies to complete a memory task. As a result the preferential use of non-spatial search strategies may have contributed to the acquisition deficit observed during memory testing.

Discussion

Increasing evidence supports the notion that a single TBI can alter the chronic neuroinflammatory environment; although few experimental studies extend beyond one year post-injury. For example, progressive cortical and hippocampal atrophy occurs in conjunction with reactive astrogliosis up to one year post-FPI in rats.[32] Similarly, glial expression of NFκ-B is observed in brain regions with persistent atrophy up to one year post-injury in the same model.[33] Even a single frontal mild TBI results in persistent deficits in attention, impulse control and decision making over 90 DPI that correlates with increased neuroinflammation in rodents.[34] These findings are consistent with human studies reporting increased mRNA expression of microglial markers OX-6 and CD68 at one year post-injury[1] and imaging studies showing increased binding of PK-[11C](R)PK11195 ligand, expressed by activated microglia, between 11 months and 17 years post-injury.[35]

The interrelationship between TBI, persistent neuroinflammation and development of AD, a prominent tauopathy, has been a topic of interest for some time. If fact, many

experimental studies have characterized the effects of TBI in various rodent models of AD in which genetic predisposition promotes the accumulation of beta-amyloid (Aβ) and MAPT pathology. Surprisingly and perhaps contrary to expected results, TBI does not significantly worsen chronic outcome in many of these models (see review[36]) and has even diminished Aβ pathology in a few studies.[37,38] Not until recently, have the neuromodulatory effects of accumulating Aβ emerged as an inflammatory stimuli in disease pathogenesis.[39] Previous work from our group demonstrates that the acute macrophage response to TBI is reduced in a genomic mouse model of AD (R1.40) prone to Aβ accumulation; however, the macrophage response persists in sub-cortical brain regions and coincides with chronic tissue loss and cognitive impairment up to 120 DPI.[25] A delayed neuroinflammatory response to TBI has also been reported by other groups examining a knock-in mouse model of AD (APP/PS1-KI). In agreement with our findings, APP/PS1-KI mice displayed a persistent neuroinflammatory response with significant cognitive impairment compared to controls.[40] We sought to extend these results by examining the neuromodulatory effects of pathogenic tau accumulation in a disease relevant mouse model of AD.

In this model, two month old hTau and B6 mice were exposed to TBI or sham injury and sacrificed at an acute and a chronic time point. The macrophage response to brain injury was significantly enhanced lateral to the site of injury and within the ipsilateral hippocampus of hTau TBI mice compared to all other groups at 3 DPI. Although not statistically significant, close examination reveals that even hTau sham mice display enhanced microglial/macrophage reactivity compared to B6 sham mice at 3 DPI in select brain regions (e.g., Fig. 1A, 1D, CD45 immunoreactivity). The presence of wild-type human tau in the absence of mouse tau is sufficient to induce age-related tau pathology, behavioral impairment, and cell loss in hTau mice[15]. Thus, these results provide evidence that hTau mice are subsequently vulnerable to a hyperactive acute microglial/macrophage response to an additional immune challenge such as TBI or even sham injury. TBI induced tau phosphorylation in the cortex lateral to the site of injury but no significant differences were identified between groups at 3 DPI. Several AT180+ cells were identified in layer 2/3 of the ectorhinal, perirhinal, and entorhinal cortical areas as well as in the pyramidal layer of the piriform cortical area. Substantial evidence demonstrates hippocampal projections

Journal of Neurotrauma
Traumatic brain injury in hTau model mice: Enhanced acute macrophage response and altered long-term recovery
 (DOI: 10.1089/neu.2017.5203)
This paper has been peer-reviewed and accepted for publication, but has yet to undergo copyediting and proof correction. The final published version may differ from this proof.

to these cortical areas,[41] and may explain why hTau TBI mice display increased AT180 immunoreactivity in this area. Importantly though, a genotype effect in AT180 immunoreactivity was identified in the ipsilateral temporal cortex supporting the observation that even hTau sham mice have an increased vulnerability to secondary injury cascades.

The cortical microglial/macrophage response to TBI as identified via CD45, F4/80, and CD68 immunohistochemistry substantially declined by 135 DPI (F4/80 and CD68 not shown). Consistent with recent observations though, a diffuse distribution of CD45+ cells were identified in the optic tract of all mice.[42] Although visual deficits were not obvious during water maze training, this pathology might help to explain the preferential use of non-spatial search strategies employed by hTau TBI mice to complete the water maze task. A more thorough characterization of visual system damage is warranted in future studies.

The lack of unique, phenotypic markers to distinguish CNS resident microglia from peripherally derived macrophages makes it difficult to assess the individual responses of these two populations to chronic TBI. Differential levels in surface expression of CD11b and CD45 serve as consistent markers to identify resident microglia as $CD11b^{+}CD45^{low/+}$ and peripheral macrophages as $Ly6C^{+}CD11b^{+}CD45^{high}$. It has been demonstrated that under inflammatory conditions, a proportion of microglia can upregulate CD45 expression to levels that are intermediate ($CD45^{int}$) between the $CD45^{low}$ microglia and $CD45^{high}$ macrophages that are often reported in the literature[43]. In an effort to identify CD45+ reactive microglia and infiltrating macrophages present in the brain at 135 DPI, we performed flow cytometric analysis. Four distinct populations were identified, including 1) $CD11b^{low}/CD45^{low}$ microglia, 2) $CD11b^{high}/CD45^{low}$ microglia, 3) $CD11b^{+}/CD45^{int}$ microglia, and 4) $Ly6C^{+}CD11b^{+}/CD45^{high}$ macrophages. $CD11b^{+}/CD45^{high}$ macrophages were also Ly6C+[44] and make up a much smaller proportion of cells in the brain compared to microglia. We predict that $Ly6C^{low}/CD11b^{+}/CD45^{high}$ cells represent $Cx3cr1^{+}$ patrolling macrophages;[45] however, a detailed analysis of Cx3cr1 expression was not included in these studies and should be considered in future experiments. Furthermore, only $CD11b^{+}/CD45^{int}$ microglia were also Ly6C+ suggesting that this population might represent inflammatory CCR2+ monocyte-derived macrophages, differentiating in the CNS tissue

environment. Again, a thorough analysis of key chemokines, Cx3cr1 and CCR2, would provide valuable insight to the cellular composition of reactive cells in the brain at 135 DPI.

Region specific tau phosphorylation was detected lateral to the injury site and in the ipsilateral temporal cortex of hTau TBI mice. hTau TBI mice also showed increased number of Gallyas-positive neurons in the ipsilateral hippocampus. A similar temporal distribution of tau pathology was not detected in any other experimental group at 135 DPI. Collectively, these data suggest that the acute microglial/macrophage response to TBI in hTau mice could result in long-term consequences that alter tau pathology. Conversely, presence of human tau in hTau mice may actively, with some unknown mechanism(s), facilitate macrophage activation for a prolonged period of time post-trauma. A direct mechanism for this relationship is not yet evident, but future studies could address the cell specific role of microglia as well as monocytes in promoting post-injury tau pathology in hTau mice via inclusion of *Cx3cr1-/- and/or Ccr2-/- mice.*[19]

Finally, a battery of behavioral tests confirmed that the moderate severity of TBI utilized in these studies did not induce global deficits in motor or cognitive function through 135 DPI. Importantly though, hTau TBI mice displayed significantly longer latencies to reach the goal platform on day one of memory testing in the water maze compared to B6 sham and TBI mice. Although hTau TBI mice consistently took longer than all other groups to reach the goal platform throughout testing, no other significant differences were detected. A single probe trial was completed at the end of memory testing. During this trial, the platform is removed and animals are given 30 seconds to swim throughout the pool. Animals that have successfully learned the task spend more time in the goal quadrant than any other quadrant. The probe trial data did not support the notion that any group had displayed true spatial memory, as the average amount of time spent in the goal quadrant was around seven seconds. These data prompted us to consider how search strategy affected completion of the memory task. Based on previous reports, we predicted that a more effective search strategy would account for the mild performance differences between groups.[27]

Swim path analysis revealed that B6 and hTau mice utilized spatial, non-spatial, and looping search strategies to locate the submerged goal platform and the use of each strategy changed over time. Notably, hTau TBI mice demonstrated a preferential use of

the non-spatial scanning search strategy compared to other groups. hTau mice regardless of injury group also displayed increased use of looping strategies across five days of memory testing compared to B6 mice. Together, these data imply that hTau mice utilize non-spatial search strategies more frequently than B6 mice. Furthermore, TBI restricts the non-spatial search path to the center of the pool in hTau mice. Together, these data imply that TBI promotes the use of non-spatial search strategies in hTau mice which might account for longer latencies to reach the submerged goal platform. These results confirm that search strategy is complex and should be considered when analyzing data from the water maze memory task. Inclusion of swim path analysis may be particularly useful when it is difficult to identify the influence of cognitive, sensory or motor function on water maze performance.[27]

In summary, these experiments indicate that wild-type human tau alters the acute and chronic microglial/macrophage response to single TBI, promotes region specific tau pathology and mild cognitive dysfunction at a chronic time point. hTau mice have been used in multiple other brain injury studies focused on the effects of repetitive TBI.[10,20,46,47] This study further supports the use of hTau mice as a disease relevant model for defining the inter-relationship between brain injury, neuroinflammation and tau pathology. This model can now be manipulated to decipher causal interactions between post-injury neuroinflammation, MAPT pathology and behavioral impairment to identify potential points of intervention to improve recovery following TBI. Collectively, these data highlight the importance of communication between MAPT and microglial/macrophages after brain injury and implicate accumulating tau as a likely neuromodulator. Moreover, these experiments suggest that an altered neuroinflammatory environment following TBI may be an important mediating factor in development of post-injury neurodegenerative disease such as AD.

Acknowledgements

This work was supported by the Department of Defense and National Institutes of Health (W81XWH-12-1-0629, BTL; R21NS077089, R01NS083704, R21NS093442, K.B.). We thank the Rodent Behavioral Core and the Flow Cytometry Core at the Lerner Research Institute within the Cleveland Clinic for technical advice and support. We thank Dr. Imad Najm for

use of the fluid percussion device. Author contributions: O.K-C. designed, performed, and analyzed all experiments and wrote the manuscript; M.S. performed surgeries, TBI's, and flow cytometry experiments; S.P. analyzed all flow cytometry data and assisted in interpretation of results; S.B. performed silver staining and assisted with biochemical analysis of data; A.K. performed immunohistochemistry and assisted with data analysis; Y-S.L. provided expertise in use of the fluid percussion device and analysis of data. K.B. provided expertise in use of the hTau mouse model and analysis of data; R.M.R. provided funding and expertise in data analysis and interpretation; B.T.L. provided funding and expertise and co-edited the manuscript.

Author Disclosure Statement

No competing financial interests exist.

References:

1. Johnson, V.E., Stewart, J.E., Begbie, F.D., Trojanowski, J.Q., Smith, D.H., and Stewart, W. (2013). Inflammation and white matter degeneration persist for years after a single traumatic brain injury. Brain 136, 28–42.

2. Goldstein, L.E., Fisher, A.M., Tagge, C.A., Zhang, X.-L., Velisek, L., Sullivan, J.A., Upreti, C., Kracht, J.M., Ericsson, M., Wojnarowicz, M.W., Goletiani, C.J., Maglakelidze, G.M., Casey, N., Moncaster, J.A., Minaeva, O., Moir, R.D., Nowinski, C.J., Stern, R.A., Cantu, R.C., Geiling, J., Blusztajn, J.K., Wolozin, B.L., Ikezu, T., Stein, T.D., Budson, A.E., Kowall, N.W., Chargin, D., Sharon, A., Saman, S., Hall, G.F., Moss, W.C., Cleveland, R.O., Tanzi, R.E., Stanton, P.K., and McKee, A.C. (2012). Chronic traumatic encephalopathy in blast-exposed military veterans and a blast neurotrauma mouse model. Sci. Transl. Med. 4, 134ra60.

3. Collins-Praino, L.E., and Corrigan, F. (2016). Does neuroinflammation drive the relationship between tau hyperphosphorylation and dementia development following traumatic brain injury? Brain. Behav. Immun. .

4. Lee, Y.-K., Hou, S.-W., Lee, C.-C., Hsu, C.-Y., Huang, Y.-S., and Su, Y.-C. (2013). Increased risk of dementia in patients with mild traumatic brain injury: a nationwide cohort study. PLoS One 8, e62422.

5. Holtzman, D.M., Carrillo, M.C., Hendrix, J.A., Bain, L.J., Catafau, A.M., Gault, L.M., Goedert, M., Mandelkow, E., Mandelkow, E.-M., Miller, D.S., Ostrowitzki, S., Polydoro, M., Smith, S., Wittmann, M., and Hutton, M. (2016). Tau: From research to clinical development. Alzheimer's Dement. 12, 1033–1039.

6. Ballatore, C., Lee, V.M.-Y., and Trojanowski, J.Q. (2007). Tau-mediated neurodegeneration in Alzheimer's disease and related disorders. Nat. Rev. Neurosci. 8, 663–72.

7. Miyasaka, T., Sato, S., Tatebayashi, Y., and Takashima, A. (2010). Microtubule destruction induces tau liberation and its subsequent phosphorylation. FEBS Lett. 584, 3227–32.

8. Başkaya, M.K., Rao, A.M., Doğan, A., Donaldson, D., and Dempsey, R.J. (1997). The biphasic opening of the blood-brain barrier in the cortex and hippocampus after traumatic brain injury in rats. Neurosci. Lett. 226, 33–6.

9. Morganti-Kossmann, M.C., Satgunaseelan, L., Bye, N., and Kossmann, T. (2007). Modulation of immune response by head injury. Injury 38, 1392–400.

10. Ojo, J.-O., Mouzon, B., Greenberg, M.B., Bachmeier, C., Mullan, M., and Crawford, F. (2013). Repetitive mild traumatic brain injury augments tau pathology and glial activation in aged hTau mice. J. Neuropathol. Exp. Neurol. 72, 137–51.

11. Tran, H.T., LaFerla, F.M., Holtzman, D.M., and Brody, D.L. (2011). Controlled cortical impact traumatic brain injury in 3xTg-AD mice causes acute intra-axonal amyloid-β accumulation and independently accelerates the development of tau abnormalities. J. Neurosci. 31, 9513–25.

12. Dressler, J., Hanisch, U., Kuhlisch, E., and Geiger, K.D. (2007). Neuronal and glial apoptosis in human traumatic brain injury. Int. J. Legal Med. 121, 365–75.

13. Neumann, H., Kotter, M.R., and Franklin, R.J.M. (2009). Debris clearance by microglia: an essential link between degeneration and regeneration. Brain 132, 288–95.

14. Gyoneva, S., Kim, D., Katsumoto, A., Kokiko-Cochran, O.N., Lamb, B.T., and Ransohoff, R.M. (2015). Ccr2 deletion dissociates cavity size and tau pathology after mild traumatic brain injury. J. Neuroinflammation 12, 228.

15. Andorfer, C., Kress, Y., Espinoza, M., de Silva, R., Tucker, K.L., Barde, Y.-A., Duff, K., and Davies, P. (2003). Hyperphosphorylation and aggregation of tau in mice expressing normal human tau isoforms. J. Neurochem. 86, 582–90.

16. Polydoro, M., Acker, C.M., Duff, K., Castillo, P.E., and Davies, P. (2009). Age-Dependent Impairment of Cognitive and Synaptic Function in the htau Mouse Model of Tau Pathology. J. Neurosci. 29, 10741–10749.

17. Andorfer, C., Acker, C.M., Kress, Y., Hof, P.R., Duff, K., and Davies, P. (2005). Cell-

Journal of Neurotrauma
Traumatic brain injury in hTau model mice: Enhanced acute macrophage response and altered long-term recovery
 (DOI: 10.1089/neu.2017.5203)
This paper has been peer-reviewed and accepted for publication, but has yet to undergo copyediting and proof correction. The final published version may differ from this proof.

cycle reentry and cell death in transgenic mice expressing nonmutant human tau isoforms. J. Neurosci. 25, 5446–54.

18. Duff, K., Knight, H., Refolo, L.M., Sanders, S., Yu, X., Picciano, M., Malester, B., Hutton, M., Adamson, J., Goedert, M., Burki, K., and Davies, P. (2000). Characterization of pathology in transgenic mice over-expressing human genomic and cDNA tau transgenes. Neurobiol. Dis. 7, 87–98.

19. Gyoneva, S., and Ransohoff, R.M. (2015). Inflammatory reaction after traumatic brain injury: therapeutic potential of targeting cell–cell communication by chemokines. Trends Pharmacol. Sci. 36, 471–480.

20. Ojo, J.O., Mouzon, B., Algamal, M., Leary, P., Lynch, C., Abdullah, L., Evans, J., Mullan, M., Bachmeier, C., Stewart, W., and Crawford, F. (2016). Chronic Repetitive Mild Traumatic Brain Injury Results in Reduced Cerebral Blood Flow, Axonal Injury, Gliosis, and Increased T-Tau and Tau Oligomers. J. Neuropathol. Exp. Neurol. 75, 636–55.

21. Bhaskar, K., Konerth, M., Kokiko-Cochran, O.N., Cardona, A., Ransohoff, R.M., and Lamb, B.T. (2010). Regulation of tau pathology by the microglial fractalkine receptor. Neuron 68, 19–31.

22. Maphis, N., Xu, G., Kokiko-Cochran, O.N., Jiang, S., Cardona, A., Ransohoff, R.M., Lamb, B.T., and Bhaskar, K. (2015). Reactive microglia drive tau pathology and contribute to the spreading of pathological tau in the brain. Brain 138, 1738–55.

23. Maphis, N., Jiang, S., Xu, G., Kokiko-Cochran, O.N., Roy, S.M., Van Eldik, L.J., Watterson, D.M., Lamb, B.T., and Bhaskar, K. (2016). Selective suppression of the α isoform of p38 MAPK rescues late-stage tau pathology. Alzheimers. Res. Ther. 8, 54.

24. Komuro, Y., Xu, G., Bhaskar, K., and Lamb, B.T. (2015). Human tau expression reduces adult neurogenesis in a mouse model of tauopathy. Neurobiol. Aging 36, 2034–2042.

25. Kokiko-Cochran, O., Ransohoff, L., Veenstra, M., Lee, S., Saber, M., Sikora, M.,

Journal of Neurotrauma
Traumatic brain injury in hTau model mice: Enhanced acute macrophage response and altered long-term recovery
 (DOI: 10.1089/neu.2017.5203)
This paper has been peer-reviewed and accepted for publication, but has yet to undergo copyediting and proof correction. The final published version may differ from this proof.

Teknipp, R., Xu, G., Bemiller, S., Wilson, G., Crish, S., Bhaskar, K., Lee, Y.-S., Ransohoff, R.M., and Lamb, B.T. (2016). Altered Neuroinflammation and Behavior after Traumatic Brain Injury in a Mouse Model of Alzheimer's Disease. J. Neurotrauma 33, 625–40.

26. Saber, M., Kokiko-Cochran, O., Puntambekar, S.S., Lathia, J.D., and Lamb, B.T. (2016). Triggering Receptor Expressed on Myeloid Cells 2 Deficiency Alters Acute Macrophage Distribution and Improves Recovery after Traumatic Brain Injury. J. Neurotrauma .

27. Brody, D.L., and Holtzman, D.M. (2006). Morris water maze search strategy analysis in PDAPP mice before and after experimental traumatic brain injury. Exp. Neurol. 197, 330–40.

28. Hsieh, C.L., Niemi, E.C., Wang, S.H., Lee, C.C., Bingham, D., Zhang, J., Cozen, M.L., Charo, I., Huang, E.J., Liu, J., and Nakamura, M.C. (2014). CCR2 deficiency impairs macrophage infiltration and improves cognitive function after traumatic brain injury. J. Neurotrauma 31, 1677–88.

29. Lin, H.-H., Stacey, M., Stein-Streilein, J., and Gordon, S. (2010). F4/80: the macrophage-specific adhesion-GPCR and its role in immunoregulation. Adv. Exp. Med. Biol. 706, 149–56.

30. Holness, C., and Simmons, D. (1993). Molecular cloning of CD68, a human macrophage marker related to lysosomal glycoproteins. Blood 81.

31. Braak, H., and Braak, E. (1991). Demonstration of amyloid deposits and neurofibrillary changes in whole brain sections. Brain Pathol. 1, 213–6.

32. Smith, D.H., Chen, X.H., Pierce, J.E., Wolf, J.A., Trojanowski, J.Q., Graham, D.I., and McIntosh, T.K. (1997). Progressive atrophy and neuron death for one year following brain trauma in the rat. J. Neurotrauma 14, 715–27.

33. Nonaka, M., Chen, X.H., Pierce, J.E., Leoni, M.J., McIntosh, T.K., Wolf, J.A., and Smith, D.H. (1999). Prolonged activation of NF-kappaB following traumatic brain

injury in rats. J. Neurotrauma 16, 1023–34.

34. Vonder Haar, C., Lam, F.C.W., Adams, W.K., Riparip, L.-K., Kaur, S., Muthukrishna, M., Rosi, S., and Winstanley, C.A. (2016). Frontal Traumatic Brain Injury in Rats Causes Long-Lasting Impairments in Impulse Control That Are Differentially Sensitive to Pharmacotherapeutics and Associated with Chronic Neuroinflammation. ACS Chem. Neurosci. .

35. Ramlackhansingh, A.F., Brooks, D.J., Greenwood, R.J., Bose, S.K., Turkheimer, F.E., Kinnunen, K.M., Gentleman, S., Heckemann, R.A., Gunanayagam, K., Gelosa, G., and Sharp, D.J. (2011). Inflammation after trauma: microglial activation and traumatic brain injury. Ann. Neurol. 70, 374–83.

36. Johnson, V.E., Stewart, W., and Smith, D.H. (2010). Traumatic brain injury and amyloid-β pathology: a link to Alzheimer's disease? Nat. Rev. Neurosci. 11, 361–70.

37. Nakagawa, Y., Nakamura, M., McIntosh, T.K., Rodriguez, A., Berlin, J.A., Smith, D.H., Saatman, K.E., Raghupathi, R., Clemens, J., Saido, T.C., Schmidt, M.L., Lee, V.M., and Trojanowski, J.Q. (1999). Traumatic brain injury in young, amyloid-beta peptide overexpressing transgenic mice induces marked ipsilateral hippocampal atrophy and diminished Abeta deposition during aging. J. Comp. Neurol. 411, 390–8.

38. Nakagawa, Y., Reed, L., Nakamura, M., McIntosh, T.K., Smith, D.H., Saatman, K.E., Raghupathi, R., Clemens, J., Saido, T.C., Lee, V.M., and Trojanowski, J.Q. (2000). Brain trauma in aged transgenic mice induces regression of established abeta deposits. Exp. Neurol. 163, 244–52.

39. Grant, J.L., Ghosn, E.E.B., Axtell, R.C., Herges, K., Kuipers, H.F., Woodling, N.S., Andreasson, K., Herzenberg, L.A., Herzenberg, L.A., and Steinman, L. (2012). Reversal of paralysis and reduced inflammation from peripheral administration of β-amyloid in TH1 and TH17 versions of experimental autoimmune encephalomyelitis. Sci. Transl. Med. 4, 145ra105.

40. Webster, S.J., Van Eldik, L.J., Watterson, D.M., and Bachstetter, A.D. (2015). Closed head injury in an age-related Alzheimer mouse model leads to an altered

neuroinflammatory response and persistent cognitive impairment. J. Neurosci. 35, 6554–69.

41. van Groen, T., Miettinen, P., and Kadish, I. (2003). The entorhinal cortex of the mouse: Organization of the projection to the hippocampal formation. Hippocampus 13, 133–149.

42. Bolton Hall, A.N., Joseph, B., Brelsfoard, J.M., and Saatman, K.E. (2016). Repeated Closed Head Injury in Mice Results in Sustained Motor and Memory Deficits and Chronic Cellular Changes. PLoS One 11, e0159442.

43. Sedgwick, J.D., Schwender, S., Imrich, H., Dörries, R., Butcher, G.W., and ter Meulen, V. (1991). Isolation and direct characterization of resident microglial cells from the normal and inflamed central nervous system. Proc. Natl. Acad. Sci. U. S. A. 88, 7438–42.

44. Geissmann, F., Manz, M.G., Jung, S., Sieweke, M.H., Merad, M., and Ley, K. (2010). Development of Monocytes, Macrophages, and Dendritic Cells. Science (80-.). 327.

45. Katsumoto, A., Lu, H., Miranda, A.S., and Ransohoff, R.M. (2014). Ontogeny and functions of central nervous system macrophages. J. Immunol. 193, 2615–21.

46. Tzekov, R., Phifer, J., Myers, A., Mouzon, B., and Crawford, F. (2016). Inflammatory changes in optic nerve after closed-head repeated traumatic brain injury: Preliminary study. Brain Inj. 30, 1428–1435.

47. Ojo, J.O., Bachmeier, C., Mouzon, B.C., Tzekov, R., Mullan, M., Davies, H., Stewart, M.G., and Crawford, F. (2015). Ultrastructural Changes in the White and Gray Matter of Mice at Chronic Time Points After Repeated Concussive Head Injury. J. Neuropathol. Exp. Neurol. 74, 1012–35.

Journal of Neurotrauma
Traumatic brain injury in hTau model mice: Enhanced acute macrophage response and altered long-term recovery
 (DOI: 10.1089/neu.2017.5203)
This paper has been peer-reviewed and accepted for publication, but has yet to undergo copyediting and proof correction. The final published version may differ from this proof.

Figure Legends

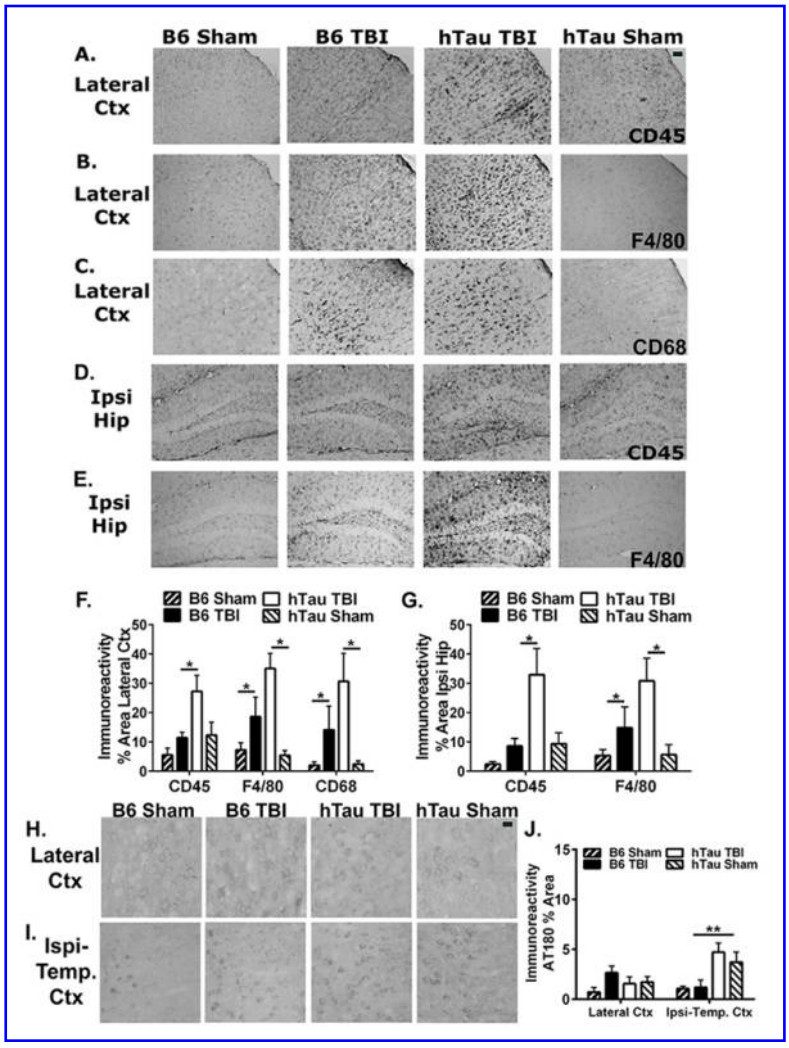

Figure 1. TBI induces enhanced microglial/macrophage response and distal tau phosphorylation in hTau mice at 3 DPI. (A-C) Representative images of CD45, F4/80, and CD68 immunostaining in sham and TBI mice in lateral cortex (ctx) at 3 DPI. (F) Quantification of percent area covered by CD45 (two way ANOVA, genotype effect $F(1, 18) = 7.445$, $p = 0.01$; injury effect , $F(1, 18) = 6.265$, $p = 0.02$; subsequent t test confirmed CD45 immunoreactivity increased in hTau TBI mice [$M = 27.28$, $SEM = 5.416$] compared to B6 TBI mice [$M = 11.41$, $SEM = 1.866$], $t(2.77) = 6.11$, $p = 0.03$), F4/80 (two-way ANOVA, injury effect $F(1, 18) = 25.03$, $p < 0.001$; interaction effect, $F(1, 18) = 5.019$, $p = 0.04$) and CD 68 (two way ANOVA, injury effect $F(1, 13) = 5.935$, $p = 0.03$) confirmed that the TBI induced microglia/macrophage response is enhanced in hTau TBI mice compared to

Journal of Neurotrauma
Traumatic brain injury in hTau model mice: Enhanced acute macrophage response and altered long-term recovery
 (DOI: 10.1089/neu.2017.5203)
This paper has been peer-reviewed and accepted for publication, but has yet to undergo copyediting and proof correction. The final published version may differ from this proof.

controls. (D-E) Representative images of CD45 and F4/80 in ipsilateral (ipsi) hippocampus at 3 DPI. (G) TBI significantly induced expression of CD45 (two way ANOVA, genotype effect, $F(1, 18) = 7.990$, $p = 0.01$); injury, $F(1, 18) = 7.209$, $p = 0.01$; subsequent t test confirmed that CD45 immunoreactivity significantly increased in hTau TBI mice [$M = 32.94$, $SEM = 8.945$] compared to B6 TBI mice [$M = 8.575$, $SEM = 2.674$], $t(2.61) = 5.86$, $p = 0.04$). (H-I) Representative images of AT180 in lateral ctx and ipsilateral temporal cortex (ipsi-temp ctx) at 3 DPI. (J) Although an interaction effect in AT180 immunoreactivity was approaching significance following two way ANOVA ($p = 0.09$) in the lateral ctx, no significant differences were identified between groups. Instead, a significant genotype effect in AT180 immunoreactivity was identified in the ipsi-temp ctx ($F(1, 16) = 14.10$, $p = 0.001$). Scale bar represents 20µm. Error bars indicate standard error of the mean (SEM); *, $p < 0.05$.

Journal of Neurotrauma
Traumatic brain injury in hTau model mice: Enhanced acute macrophage response and altered long-term recovery
 (DOI: 10.1089/neu.2017.5203)
This paper has been peer-reviewed and accepted for publication, but has yet to undergo copyediting and proof correction. The final published version may differ from this proof.

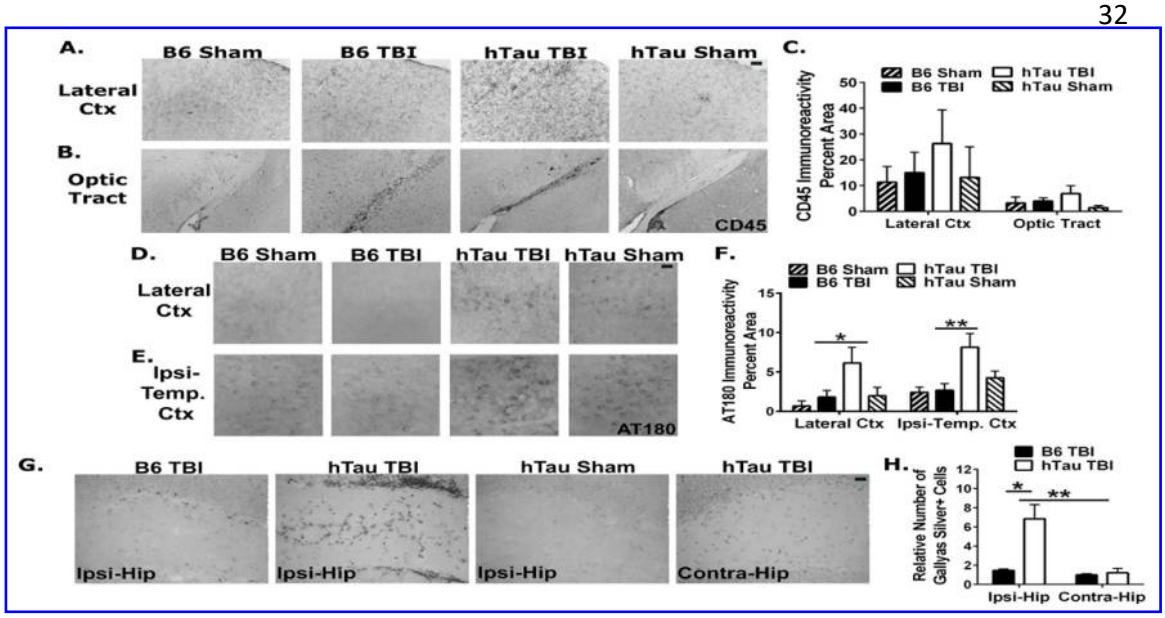

Figure 2. TBI induced microglial/macrophage reactivity declines but region specific tau pathology persists in hTau TBI mice at 135 DPI. (A-B) Representative images of CD45 immunostaining in sham and TBI mice in lateral ctx and optic tract at 135 DPI. (C) No significant differences in CD45 immunostaining in the lateral ctx or optic tract were detected between groups. (D-E) Representative images of AT180 immunostaining in sham and TBI mice in lateral ctx and ipsi-temp ctx at 135 DPI. (F) TBI significantly increased AT180 immunoreactivity in hTau TBI mice compared to all other groups in the lateral ctx (two way ANOVA, genotype effect, $F(1, 19) = 4.752$, $p < 0.05$) and in the ipsi-temp ctx (two-way ANOVA, genotype effect, $F(1, 19) = 10.11$, $p < 0.01$). A significant difference in AT180 immunoreactivity was detected between B6 ($M = 1.81$, $SEM = 0.866$) and hTau TBI ($M = 6.14$, $SEM = 1.973$) mice in the ipsi-temp ctx ($t(10) = 2.836$, $p < 0.05$), but no difference was detected between hTau TBI and hTau sham mice ($M = 1.983$, $SEM = 1.059$). (G) Representative images of silver staining in hippocampi in B6 and hTau mice at 135 DPI. (H) Silver staining was significantly enhanced in the ipsi-hip of hTau TBI mice compared to B6 TBI mice (cell counts normalized to B6 TBI contra-hip; two way ANOVA, genotype effect, $F(1, 8) = 12.58$, $p < 0.01$; hemisphere effect, $F(1, 8) = 14.94$, $p < 0.01$; interaction effect, $F(1, 8) = 10.69$, $p < 0.05$). Scale bar represents 20µm. Error bars indicate SEM; *, $p < 0.05$; **, $p < 0.01$.

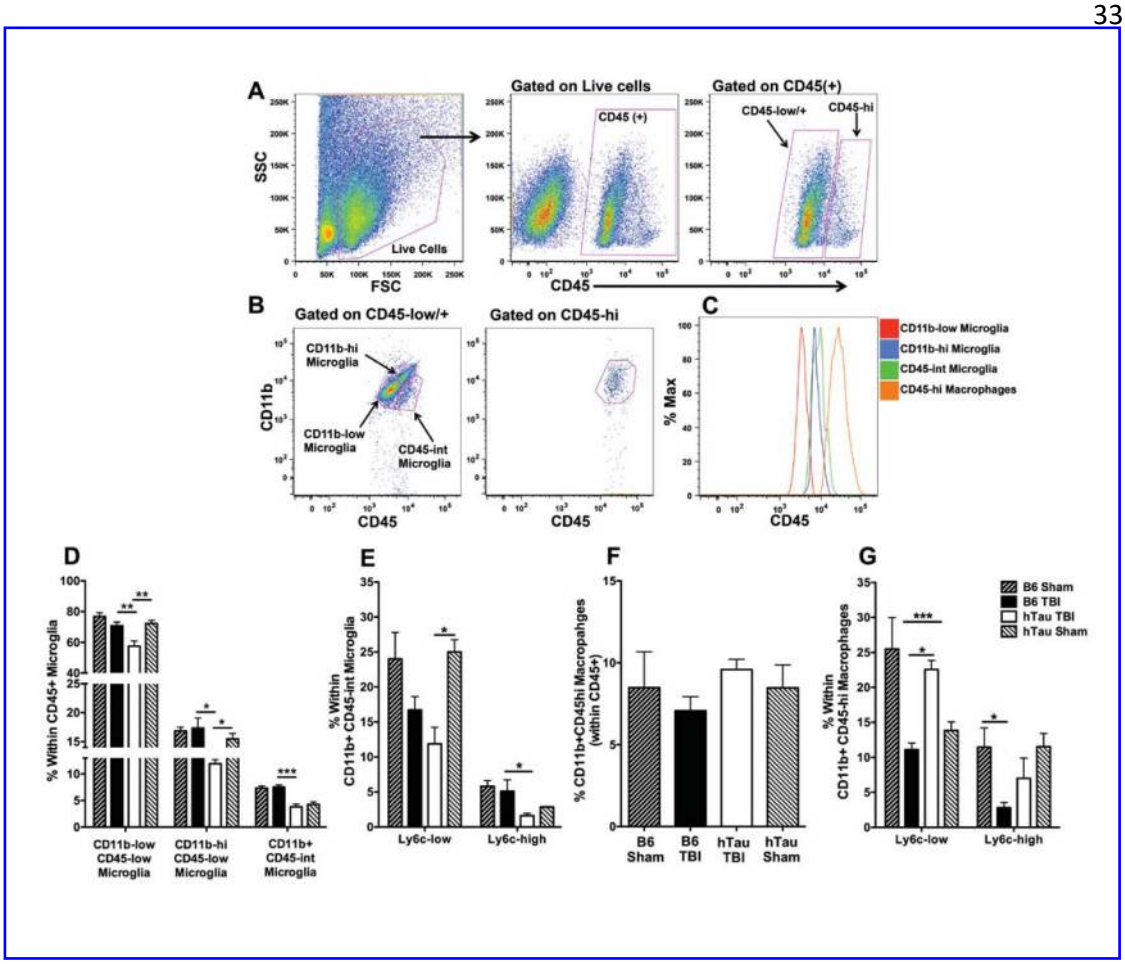

Figure 3. Differential modulation of immune responses of brain resident microglia vs. peripheral macrophages at 135 DPI. (A) Representative scatterplots showing the gating strategy used to distinguish CD45-low and CD45-hi populations from the CNS of mice at 135 DPI. (B) Representative scatterplots identifying distinct microglial and macrophage subpopulations based on relative expression of surface markers CD11b and CD45. Two distinct populations of microglia, namely those with low (CD11b-low) and high (CD11b-high) CD11b expression and a third subset with an intermediate level of CD45 (CD45-int) were identified within the CD45-low/+ population. A distinct population of CD11b(+) cells was identified as peripheral macrophages within the CD45-high cells. (C) Representative histogram overlays show that individual myeloid cell populations identified express differential levels of CD45. (D) Quantitation of the relative proportions of different microglial subsets identified in (B) revealed a significant reduction in all three population in the hTau TBI mice as compared to injured controls (two way ANOVA CD11b-low/CD45-low

microglia, injury effect, $F(1, 18) = 16.45$, $p < 0.01$; genotype effect, $F(1, 18) = 12.22$, $p < 0.01$; post-hoc comparisons confirmed that the proportion of CD11b-low/CD45-low microglia was significantly reduced in hTau TBI mice [$M = 57.5$, $SEM = 3.37$] compared to B6 TBI mice [$M = 70.86$, $SEM = 2.32$]; $t(18) = 3.705$, $p < 0.01$; two way ANOVA CD11b-hi/CD45low microglia, genotype effect, $F(1, 18) = 6.11$, $p < 0.05$; two way ANOVA CD11b+/CD45-int microglia, genotype effect, $F(1, 18) = 48.95$, $p < 0.01$, post-hoc comparisons confirmed that the proportion of CD11b+/CD45-int microglia was significantly reduced in hTau TBI mice [$M = 3.82$, $SEM = 0.52$] compared to B6 TBI mice [$M = 7.54$, $SEM = 0.42$]; $t(18) = 5.39$, $p < 0.01$). (E) Quantitation of Ly6c-low and Ly6c-hi expressing, activated CD11b+CD45-int microglia revealed a significant injury effect in Ly6c-low expressing cells (two way ANOVA, injury effect, $F(1, 15) = 17.42$, $p < 0.01$) as well as a significant genotype effect in Ly6c-high expression cells (two way ANOVA, genotype effect, $F(1, 14) = 7.37$, $p < 0.05$). (F) Quantitation of the proportion of peripheral macrophages within the CD45(+) population revealed no difference in the sustained macrophage response (CD11b+/CD45hi) at 135 DPI. (G) Quantitation of macrophage activation revealed that while the proportion of Ly6c-low and Ly6c-high macrophages is significantly reduced in the B6 TBI as compared to B6 Sham injured animals, Ly6c-low macrophages in the hTau TBI group are significantly increased as compared to the B6 TBI and hTau sham injured animals (two way ANOVA Ly6c-low/CD11b+/CD45hi macrophages, interaction effect $F(1, 10) = 29.09$, $p < 0.01$; post-hoc comparisons confirmed that the proportion of Ly6c-low/CD11b+/CD45hi macrophages was significantly increased in hTau TBI mice [$M = 22.57$, $SEM = 1.29$] compared to B6 TBI mice [$M = 11.13$, $SEM = 0.93$]; $t(10) = 3.78$, $p < 0.05$; two way ANOVA Ly6c-hi/CD11b+/CD45hi macrophages, injury effect, $F(1, 10) = 10.34$, $p < 0.01$). All quantitation data represents n = 5-7 mice from 5 different experiments. Error bars indicate SEM; *, $p < 0.05$; **, $p < 0.01$.

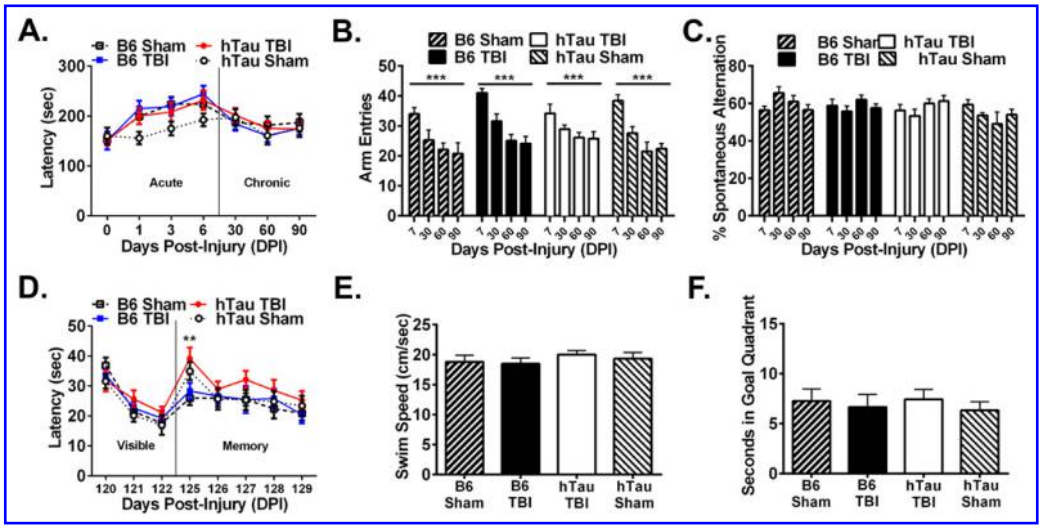

Figure 4. TBI induces spatial memory alterations in the absence of motor dysfunction in hTau TBI mice. (A) Mean latency to fall from the rotating rod was similar between sham and TBI mice at all post-injury time points. (B) Average total arm entries in the Y maze significantly decreased in all groups over time, repeated measures ANOVA , $F(3, 168) = 28.77$, $p < 0.01$. (C) Percent spontaneous alternation in the Y maze was similar between groups at all time points. (D) Latency to reach the visible platform in MWM training was similar between all groups. hTau TBI mice took significantly longer than all other groups to reach the submerged goal platform on memory testing day 1; however, latency to reach the goal platform was similar between all groups in subsequent testing days (two way repeated measures ANOVA, injury effect, $F(3, 12) = 9.51$, $p < 0.01$; testing day effect, $F(4, 48) = 5.38$, $p < 0.01$; post-hoc comparisons confirmed that hTau TBI mice [$M = 39.11$, $SEM = 3.67$] compared to B6 TBI mice [$M = 28.31$, $SEM = 2.7$]; $t(60) = 2.69$, $p < 0.05$) and B6 sham mice [$M = 21.46$, $SEM = 2.54$]; $t(60) = 3.28$, $p < 0.05$). Visible platform testing occurred 120-122 DPI and memory testing occurred 125-129 DPI. (E) Average swim speed to reach the platform in MWM testing was similar between all groups. (F) Average seconds spent in the goal quadrant during a single probe trial was similar between all groups. Error bars indicate SEM; *, $p < 0.05$; **, $p < 0.01$.

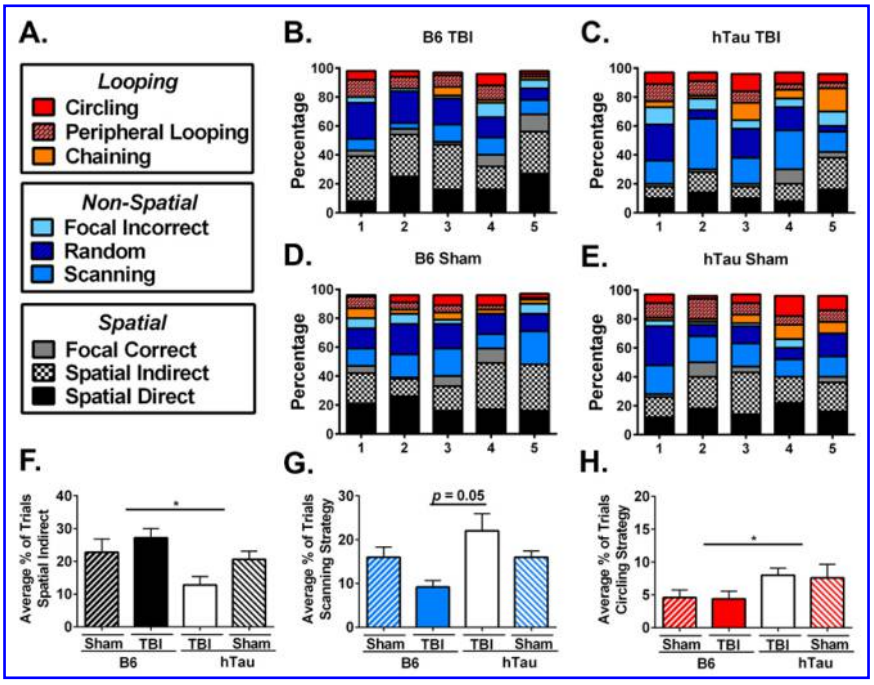

Figure 5. hTau TBI display impaired use of spatial search strategies in the MWM. (A) Graph key of spatial search strategies considered when scoring swim path in MWM. Average percentage of spatial, non-spatial and looping search strategies in (B) B6 TBI, (C) hTau TBI, (D) B6 sham, and (E) hTau sham mice across 5 days (y axis) of memory testing. hTau TBI mice demonstrate a preferential use of non-spatial search strategies across days. (F) B6 mice regardless of injury utilize the spatial indirect search strategy significantly more often than hTau mice (two way ANOVA, genotype effect, $F(1, 56) = 4.37$, $p < 0.05$). (G) hTau TBI mice rely on the scanning strategy significantly more often than B6 TBI mice; two way ANOVA, interaction effect, $F(1, 8) = 5.08$, $p = 0.05$; post-hoc comparisons confirmed that hTau TBI mice [$M = 22.0$, $SEM = 3.94$] used a scanning strategy significantly more often than B6 TBI mice [$M = 9.2$, $SEM = 1.5$]; $t(8) = 3.04$, $p < 0.05$) . (H) hTau mice regardless of injury utilize the circling strategy more often than B6 mice (two way ANOVA, genotype effect, $F(1, 56) = 11.59$, $p < 0.01$). Error bars indicate SEM; *, $p < 0.05$.